

# Ferromagnetic Instability in a Doped Band-Gap Semiconductor FeGa<sub>3</sub>

K. Umeo,<sup>1,2,\*</sup> Y. Hadano,<sup>2</sup> S. Narazu,<sup>2</sup> T. Onimaru,<sup>2</sup> M. A. Avila,<sup>3</sup> and T. Takabatake<sup>2,4</sup>

<sup>1</sup>*Cryogenics and Instrumental Analysis Division, N-BARD,  
Hiroshima University, Higashi-Hiroshima 739-8526, Japan*

<sup>2</sup>*Department of Quantum matter, AdSM,  
Hiroshima University, Higashi-Hiroshima 739-8530, Japan*

<sup>3</sup>*Centro de Ciências Naturais e Humanas,  
Universidade Federal do ABC, Santo André - SP, 09210-971, Brazil*

<sup>4</sup>*Institute for Advanced Materials Research,  
Hiroshima University, Higashi-Hiroshima 739-8530, Japan*

(Dated: March 2, 2018)

## Abstract

We report the effects of electron doping on the ground state of a diamagnetic semiconductor FeGa<sub>3</sub> with a band gap of 0.5 eV. By means of electrical resistivity, magnetization and specific heat measurements we have found that gradual substitution of Ge for Ga in FeGa<sub>3-y</sub>Ge<sub>y</sub> yields metallic conduction at a very small level of  $y = 0.006$ , then induces weak ferromagnetic (FM) order at  $y = 0.13$  with a spontaneous moment of  $0.1 \mu_B/\text{Fe}$  and a Curie temperature  $T_C = 3.3$  K, which continues increasing to  $T_C = 75$  K as doping reaches  $y = 0.41$ . The emergence of the FM state is accompanied by quantum critical behavior as observed in the specific heat,  $C/T \propto -\ln T$ , and in the magnetic susceptibility,  $M/B \propto T^{-4/3}$ . At  $y = 0.09$ , the specific heat divided by temperature  $C/T$  reaches a large value of  $70 \text{ mJ/K}^2\text{molFe}$ , twice as large as that reported on FeSi<sub>1-x</sub>Ge<sub>x</sub> for  $x_c = 0.37$  and Fe<sub>1-x</sub>Co<sub>x</sub>Sb<sub>2</sub> for  $x_c = 0.3$  at their respective FM quantum critical points. The critical concentration  $y_c = 0.13$  in FeGa<sub>3-y</sub>Ge<sub>y</sub> is quite small, despite the fact that its band gap is one order of magnitude larger than those in FeSi and FeSb<sub>2</sub>. In contrast, no FM state emerges by substituting Co for Fe in Fe<sub>1-x</sub>Co<sub>x</sub>Ga<sub>3</sub> in the whole range  $0 \leq x \leq 1$ , although both types of substitution should dope electrons into FeGa<sub>3</sub>. The FM instability found in FeGa<sub>3-y</sub>Ge<sub>y</sub> indicates that strong electron correlations are induced by the disturbance of the Fe 3d - Ga 4p hybridization.

## I. INTRODUCTION

Iron- and ruthenium-based semiconductors with band gaps of the order of 0.1 eV such as FeSi,<sup>1–15</sup> FeSb<sub>2</sub>,<sup>16–22</sup> FeGa<sub>3</sub>,<sup>23–33</sup> Fe<sub>2</sub>VAl,<sup>34</sup> RuAl<sub>2</sub>,<sup>35</sup> RuGa<sub>3</sub>,<sup>24</sup> and RuIn<sub>3</sub>,<sup>36</sup> have attracted considerable attention because of their unusual transport and magnetic behaviors. These compounds have been intensively studied not only as candidate thermoelectric materials, but also from an academic interest in the mechanism of the gap formation, which has been discussed in the context of strong correlations involving *3d* or *4d* bands, analogous to *4f* bands in rare-earth-based Kondo semiconductors. In typical *4f* Kondo semiconductors such as YbB<sub>12</sub> and Ce<sub>3</sub>Pt<sub>3</sub>Bi<sub>4</sub>, a small gap of about 0.02 eV is formed by the hybridization of localized *4f* states with the conduction bands.<sup>37</sup> Kondo semiconductors are distinguished from band-gap semiconductors on the following points: (i) The gap gradually disappears upon heating to a temperature which is lower than the gap energy, as observed in the temperature dependence of optical conductivity for FeSi and FeSb<sub>2</sub>.<sup>3,6,18</sup> (ii) The gap is strongly suppressed by substituting both the magnetic ion site and the ligand site at a low level. Thereby, the magnetization and the electronic specific heat coefficient are largely enhanced. This enhancement is observed in Fe<sub>1–x</sub>Co<sub>x</sub>Si,<sup>2,11</sup> FeSi<sub>1–x</sub>Ge<sub>x</sub>,<sup>10</sup> Fe<sub>1–x</sub>Co<sub>x</sub>Sb<sub>2</sub>,<sup>20,21</sup> and FeSb<sub>2–x</sub>Sn<sub>x</sub>.<sup>19</sup> Recently, however, the above physical properties of FeSi and FeSb<sub>2</sub> have been explained by a minimum model of covalent insulator within a single-site dynamical mean-field approximation.<sup>38</sup> Furthermore, the electronic structure of FeSi measured by photoemission experiments has no distinct features relevant to a Kondo picture, but is qualitatively explained within the band calculations by the density functional theory without many-body effects,<sup>13,39,40</sup> Therefore, it remains an issue whether FeSi and FeSb<sub>2</sub> are Kondo or usual semiconductors.

FeSi and FeSb<sub>2</sub> are nearly ferromagnetic semiconductors. In spite of the absence of magnetic order in both FeSi and CoSi, their mixed system Fe<sub>1–x</sub>Co<sub>x</sub>Si exhibits magnetic order in the range  $0.05 < x < 0.8$ .<sup>2,11</sup> Small angle neutron scattering experiments have revealed a helical spin magnetic structure with a long period of more than 300 Å.<sup>2</sup> This magnetic structure is realized by the Dzyaloshinsky-Moriya interaction as found in B20 crystal structures without inversion center. By applying magnetic fields, the helical structure easily transforms to the FM one. Moreover, FeSi<sub>1–x</sub>Ge<sub>x</sub> ( $x \geq 0.37$ ) and Fe<sub>1–x</sub>Co<sub>x</sub>Sb<sub>2</sub> ( $0.2 \leq x < 0.5$ ) also present the emergence of ferromagnetism.<sup>10,20,21</sup> According to the local density approximation plus

on-site Coulomb repulsion correction method, the semiconducting states in FeSi and FeSb<sub>2</sub> are close in energy to a FM and metallic state.<sup>5,41</sup> Thereby, local Coulomb repulsions  $U$  of 3.7 eV and 2.6 eV were obtained for FeSi and FeSb<sub>2</sub>, respectively.

FeGa<sub>3</sub> crystallizes into a tetragonal structure with space group  $P4_2/mnm$ . A narrow  $d(\text{Fe})$  -  $p(\text{Ga})$  hybridization band-gap  $E_g = 0.3 - 0.5\text{eV}$  is expected from the band structure calculations based on the density-functional theory within the local density approximation.<sup>24,26</sup> It is consistent with the observed gap of  $0.25 - 0.47\text{ eV}$  (Refs. 25, 27, 28, 32) for FeGa<sub>3</sub>. This value is one order of magnitude larger than that in FeSi (Ref. 4) and FeSb<sub>2</sub>,<sup>16</sup> whose gaps are 0.08 and 0.02 eV, respectively. In FeGa<sub>3</sub>, the absence of a significant impurity-induced density of states at the Fermi level  $E_F$  is indicated by an extremely small  $\gamma$  value of  $0.03\text{ mJ/K}^2\text{mol}$ .<sup>28</sup> These facts suggest that correlation effects or the nature of the Kondo semiconductor in FeGa<sub>3</sub> are weaker than in FeSi and FeSb<sub>2</sub>. This weak correlation effect in FeGa<sub>3</sub> manifests itself by the absence of a sharp peak at the valence band maximum just below  $E_F$ , as found in recent photoemission spectra.<sup>32</sup> The magnetic susceptibility shows diamagnetism below room temperature, and it increases exponentially with temperature above 500 K.<sup>27,28</sup> Recently, it has been reported that Co substitution for Fe in Fe<sub>1-x</sub>Co<sub>x</sub>Ga<sub>3</sub> ( $x = 0.05$ ) induces a crossover from the semiconducting state to a metallic state with weakly coupled local moments.<sup>29</sup>

In order to investigate the mechanism of metallization and emergence of ferromagnetism induced by electron doping in FeGa<sub>3</sub>, we have synthesized  $3d$  electron doped Fe<sub>1-x</sub>Co<sub>x</sub>Ga<sub>3</sub> samples and  $4p$  electron doped FeGa<sub>3-y</sub>Ge<sub>y</sub> samples and measured the electrical resistivity  $\rho$ , specific heat  $C$ , and magnetization  $M$ . Our results demonstrate a doping-induced semiconductor-metal transition in both systems, but weak FM state only in FeGa<sub>3-y</sub>Ge<sub>y</sub> for  $y \geq 0.13$ . We will discuss how the doping effects in the FeGa<sub>3</sub> system differ from those in the FeSi and FeSb<sub>2</sub> systems.

## II. EXPERIMENTAL DETAILS

Single crystals of Fe<sub>1-x</sub>Co<sub>x</sub>Ga<sub>3</sub> and FeGa<sub>3-y</sub>Ge<sub>y</sub> were grown by a Ga self-flux method. Mixtures of high purity elements in compositions Fe : Co : Ga =  $1 - X$  :  $X$  : 9 ( $0 \leq X \leq 1$ ) and Fe : Ga : Ge =  $1 : 8.5 : Y$  ( $0.01 \leq Y \leq 3$ ) were sealed in evacuated silica ampoules. The ampoules were heated to  $1100\text{ }^\circ\text{C}$  and cooled over 150 hours to  $500\text{ }^\circ\text{C}$ , at which point the

molten Ga flux was separated by decanting. The crystal compositions were determined by electron-probe microanalysis (EPMA) using a JEOL JXA-8200 analyzer. The effective Co doping levels in the crystals were found to roughly agree with the nominal composition  $X$ , whereas a maximum effective Ge doping of  $y = 0.41$  results for an initial composition  $Y = 3$ . X-ray diffraction patterns of powdered samples confirmed that all alloys for  $0 \leq x \leq 1$  and  $y \leq 0.41$  crystallized in the  $\text{FeGa}_3$ -type structure. No impurity phases in the single crystals were found by x-ray diffraction nor EPMA. The lattice parameters  $a$  and  $c$ , and the unit cell volume  $V$  are plotted in Fig. 1. The values of  $a = 6.262$  (6.240) and  $c = 6.556$  (6.439) Å of  $\text{FeGa}_3$  ( $\text{CoGa}_3$ ) are in good agreement with reported values.<sup>24, 43</sup> For  $\text{Fe}_{1-x}\text{Co}_x\text{Ga}_3$ , both  $a$  and  $c$  parameters decrease monotonically with increasing  $x$  from 0 to 1, following Vegard's law. The  $V(x = 1)$  is 2.5 % smaller than  $V(x = 0)$ . For  $\text{FeGa}_{3-y}\text{Ge}_y$ , the  $a$  value increases with increasing  $y$ , whereas the  $c$  value decreases. As a result,  $V(y = 0.41)$  is only 1% smaller than  $V(y = 0)$ .

Resistivity measurements were performed on a home-built system using a standard four-probe AC method, in the temperature range of 3 – 380 K provided by a Gifford-McMahon type refrigerator. The magnetization  $M$  was measured under ambient pressure as well as applied pressures up to 2.21 GPa by using a SQUID magnetometer (Quantum Design MPMS) from 2 to 350 K and in magnetic fields up to 5 T. To measure  $M$  down to 0.35 K, we adopted a capacitive Faraday method using a high resolution capacitive force-sensing device installed in a  $^3\text{He}$  refrigerator.<sup>43</sup> The specific heat  $C$  from 0.3 to 300 K was measured by a relaxation method on a Quantum Design PPMS.

### III. RESULTS

Figures 2(a) and (b) show the temperature dependence of  $\rho$  for  $\text{Fe}_{1-x}\text{Co}_x\text{Ga}_3$  and  $\text{FeGa}_{3-y}\text{Ge}_y$ , respectively. For  $\text{Fe}_{1-x}\text{Co}_x\text{Ga}_3$ , the data are normalized by the  $\rho$  value at 380 K. The  $\rho(T)$  data for  $x = 0$  shown in the inset of Fig. 2(a) exhibits upturns in the temperature ranges of  $T > 260$  K and  $T < 50$  K, which are attributed to intrinsic response due to the band gap of 0.5 eV, and extrinsic one due to the impurity donors, respectively.<sup>28</sup> The  $\rho(T)/\rho_{380}$  for  $x = 0.02$  increases with decreasing temperature in the entire temperature range. With increasing  $x$ , the upturn in  $\rho(T)/\rho_{380}$  is suppressed and  $\rho(T)/\rho_{380}$  for  $x \geq 0.23$  shows metallic behavior. On the other hand, the substitution of Ge for Ga in  $\text{FeGa}_{3-y}\text{Ge}_y$

at a very small level of  $y = 0.006$  yields metallic conduction. It should be recalled that for  $\text{Fe}_{1-x}\text{Co}_x\text{Si}$  and  $\text{FeSi}_{1-x}\text{Ge}_x$ , the semiconductor-metal transition occurs at high levels of substitution  $x = 0.6$  and  $0.25$ , respectively.<sup>10,11</sup> Despite the fact that the band gap of  $0.5$  eV for  $\text{FeGa}_3$  is one order of magnitude larger than the one in  $\text{FeSi}$ , metallization occurs in  $\text{FeGa}_{3-y}\text{Ge}_y$  at a much smaller doping level, suggesting that Ge substitution in  $\text{FeGa}_3$  introduces drastic changes in the electronic state.

The temperature dependence of the magnetic susceptibility  $M/B$  and its inverse  $B/M$  for  $\text{Fe}_{1-x}\text{Co}_x\text{Ga}_3$  are displayed in Figs. 3(a), (b), and (c). The diamagnetic behavior for  $x = 0$  and  $1$  suggests that the Fermi level lies in the energy gap. The  $M/B(T)$  for  $0.1 \leq x \leq 0.72$  shows Curie-Weiss paramagnetic behavior above  $50$  K. The negative value of the paramagnetic Curie temperature  $\theta_p$  for  $0.1 \leq x \leq 0.72$  implies that an antiferromagnetic interaction is dominant in this range.

On the other hand, a ferromagnetic (FM) order occurs in  $\text{FeGa}_{3-y}\text{Ge}_y$  for  $y \geq 0.13$ . As shown in Fig. 4, a spontaneous magnetic moment saturation  $\mu_s$  is observed in the magnetization curves  $M(B)$  for  $y \geq 0.13$  at  $2$  K, and the value of  $\mu_s$  increases with increasing  $y$ . However, the value of  $\mu_s$  is significantly smaller than that of Fe metal,  $2.22 \mu_B/\text{Fe}$ .<sup>44</sup> Furthermore, the  $M/B$  data as a function of temperature shows a ferromagnetic behavior for  $y \geq 0.13$  as shown in Fig. 5. This FM transition should be a bulk property because  $C(T)$  has a clear anomaly at the  $T_C$  determined by the  $M/B$  data, as shown in the inset of Fig. 5.

Figure 6 shows the temperature dependence of inverse magnetic susceptibility  $B/M$  of  $\text{FeGa}_{3-y}\text{Ge}_y$ . For  $y \geq 0.08$ , the  $B/M$  data follow the Curie-Weiss law. The value of  $\theta_p$  for  $y \leq 0.09$  is negative, and changes to positive for  $y \geq 0.13$ . Both  $\theta_p$  and Curie temperature  $T_C$  as a function of  $y$  are displayed in the upper panel of the inset of Fig. 6. The  $T_C$  was estimated as the temperature where the extrapolation of  $M(T)^2$  becomes zero. The increase in both  $\theta_p$  and  $T_C$  with increasing  $y$  indicates that the FM interaction is enhanced by Ge doping.

In order to study the nature of ferromagnetism in  $\text{FeGa}_{3-y}\text{Ge}_y$  for  $y \geq 0.13$ , the pressure dependence of  $M$  has been measured. Figure 7 shows the temperature dependence of  $M/B$  for  $y = 0.34$  under various pressures  $P$  and the inset shows the pressure dependence of  $T_C$ . It is found that  $T_C$  decreases as  $T_C \propto P^{3/4}$  which is predicted by the spin-fluctuation theory.<sup>45</sup> Furthermore, as shown in the lower panel of the inset of Fig. 6, the ratio of  $\mu_{eff}/\mu_s$  is as

high as 4 – 10. These findings suggest that  $\text{FeGa}_{3-y}\text{Ge}_y$  for  $y \geq 0.13$  is an itinerant weak ferromagnet.

The specific heat divided by temperature,  $C/T$ , as a function of  $T^2$  for  $\text{Fe}_{1-x}\text{Co}_x\text{Ga}_3$  and  $\text{FeGa}_{3-y}\text{Ge}_y$  is shown in Fig. 8. The  $C/T$  data of  $\text{FeGa}_{3-y}\text{Ge}_y$  for  $0.05 \leq y \leq 0.15$  displays an upturn below 5 K. The electronic specific-heat coefficient  $\gamma$  was estimated by the extrapolation of the  $C/T$  data to  $T = 0$ . The variations of  $T_C(y)$  for  $\text{FeGa}_{3-y}\text{Ge}_y$  and  $\gamma$  ( $x$  and  $y$ ) for  $\text{Fe}_{1-x}\text{Co}_x\text{Ga}_3$  and  $\text{FeGa}_{3-y}\text{Ge}_y$  are shown in Figs. 9 (a) and (b). It is worth noting that  $\gamma(y)$  exhibits a sharp peak of 70 mJ/K<sup>2</sup>mol at  $y = 0.09$  near the critical concentration  $y_c = 0.13$  where the ground state changes from a nonmagnetic state to a FM state, clearly contrasting with the almost flat behavior in  $\gamma(x)$  for  $\text{Fe}_{1-x}\text{Co}_x\text{Ga}_3$ . The value of 70 mJ/K<sup>2</sup>mol for  $\gamma(y = 0.09)$  is enhanced by a factor of 2300 compared to  $\gamma(y = 0) = 0.03$  mJ/K<sup>2</sup>mol, indicating the appearance of a heavy-fermion state in the vicinity of the FM instability.

The FM quantum critical behavior in  $C/T$  and  $M/B$  for  $\text{FeGa}_{3-y}\text{Ge}_y$  ( $y = 0.09$ ) are evidenced in the plots in Fig. 10. The specific heat and magnetic susceptibility for  $y = 0.09$  follow the functional forms of  $C/T \propto -\ln T$  and  $M/B \propto T^{-4/3}$ , which are predicted by the self-consistent renormalization (SCR) theory for FM spin fluctuations in three dimensional systems.<sup>46</sup> These observations are consistent with the pressure dependence of  $T_C \propto P^{3/4}$  in Fig. 7. On the other hand, as shown in Fig. 11, the  $T$ -linear dependence of  $\rho(T)$  resistivity near the critical concentration of  $y = 0.15$  is at variance with the  $T^{5/3}$  dependence predicted by the SCR theory. The  $\rho(T)$  data for  $y = 0.08$  at  $T < 30$  K obeys  $T^{1.9}$ , which indicates the recovery of the Fermi-liquid state. We will discuss the quantum critical behavior in  $\text{FeGa}_{3-y}\text{Ge}_y$  in the next section.

#### IV. DISCUSSIONS

We now compare the doping effects on the electronic and magnetic states in  $\text{Fe}_{1-x}\text{Co}_x\text{Ga}_3$  and  $\text{FeGa}_{3-y}\text{Ge}_y$  with those in the FeSi and FeSb<sub>2</sub> systems. For  $\text{Fe}_{1-x}\text{Co}_x\text{Ga}_3$ , the semiconductor-metal transition occurs at  $x = 0.23$ , whereas no magnetically ordered state is induced in the whole range  $0 \leq x \leq 1$ . The gradual and weak change of  $\gamma(x)$  for  $\text{Fe}_{1-x}\text{Co}_x\text{Ga}_3$  suggests that the band structure changes in the rigid-band frame. A similar situation has been observed in  $\text{Fe}_{1-x}\text{Co}_x\text{Si}$ , which exhibits a helical magnetically ordered

state in the range  $0.05 \leq x < 0.8$ .<sup>11</sup> A photoemission study on  $\text{Fe}_{1-x}\text{Co}_x\text{Si}$  revealed that the  $x$  dependence of the band structure near the Fermi level is described by the rigid-band model.<sup>47</sup> Therefore, the Stoner criterion can be applied to describe the magnetism of  $\text{Fe}_{1-x}\text{Co}_x\text{Ga}_3$  and  $\text{Fe}_{1-x}\text{Co}_x\text{Si}$ . The criterion for the ferromagnetic state is given by the relation  $UD(\varepsilon_F) \geq 1$ , where  $U$  and  $D(\varepsilon_F)$  are Coulomb repulsion and the density of states (DOS) at the Fermi level, respectively.<sup>44</sup> From a photoemission spectroscopy study of  $\text{FeGa}_3$ , the magnitude of  $U$  was estimated as 3 eV, which is comparable with 3.7 eV for  $\text{FeSi}$ .<sup>5,32</sup> Therefore, the absence of a magnetically ordered state in  $\text{Fe}_{1-x}\text{Co}_x\text{Ga}_3$  is a result of the fact that  $D(\varepsilon_F)$  at the bottom of the conduction band for  $\text{Fe}_{1-x}\text{Co}_x\text{Ga}_3$  is smaller than that for  $\text{Fe}_{1-x}\text{Co}_x\text{Si}$ .

On the other hand, for  $\text{FeGa}_{3-y}\text{Ge}_y$ , electron doping at a small level  $y = 0.006$  already induces the semiconductor-metal transition. The Ga site substitution disturbs the  $3d$ - $4p$  hybridization, which should lead to a dramatic change in the electronic state. Higher doping for  $y \geq 0.13$  yields a FM order. The doping induced FM state in the analogous system  $\text{FeSi}_{1-x}\text{Ge}_x$  was explained by a mean-field slave-boson approach.<sup>10,48</sup> Thereby, the key parameter driving the magnetic phases is ratio between the Coulomb repulsion  $U$  and the hybridization of the localized-conduction electrons  $V$ . With increasing  $U/V$ , the paramagnetic ground state changes into an antiferromagnetic state and furthermore a FM state.<sup>48</sup> For  $\text{FeGa}_{3-y}\text{Ge}_y$ , the disturbance of the ligand Ga/Ge site may lead to the suppression of the  $d$ - $p$  hybridization  $V$ , whereas  $U$  in the Fe 3d shell would remain unchanged. Therefore, the Ga site substitution can yield the increase of  $U/V$  and thus induce a FM ground state. On the other hand, for  $\text{Fe}_{1-x}\text{Co}_x\text{Ga}_3$ , the Fermi level shifts maintaining a rigid band, whereby  $V$  does not change. Because  $U/V$  is almost constant against  $x$ , no magnetic order is realized. Very recently, the experimental data for resistivity, specific heat and magnetization of  $\text{FeSi}_{1-x}\text{Ge}_x$  have been explained by a minimal microscopic model.<sup>14,15</sup> It is highly desirable to study whether this microscopic model is applicable for  $\text{FeGa}_{3-y}\text{Ge}_y$ .

Next, we focus on the FM quantum critical behavior (QCB) in  $\text{FeGa}_{3-y}\text{Ge}_y$ . Although ferromagnetic or antiferromagnetic QCB has been observed in many  $f$ -electron systems,<sup>49</sup> the FM QCB in  $d$ -transition metal systems has been identified on a much smaller number of compounds, such as  $\text{ZrZn}_2$  (Ref. 50) and  $\text{Ni}_x\text{Pd}_{1-x}$ .<sup>51</sup> The FM QCB in these systems has been explained in terms of the SCR theory.<sup>46</sup> For  $\text{FeGa}_{3-y}\text{Ge}_y$ , the experimental results of  $C(T)$  and  $M(T)/B$  near the critical concentration are consistent with the SCR theory of FM

spin fluctuations, whereas the  $T$ -linear resistivity is at variance with the  $T^{5/3}$  dependence predicted by this theory. Interestingly,  $\text{Fe}_{0.7}\text{Co}_{0.3}\text{Si}$  shows  $T$ -linear resistivity under the critical pressure of 7 GPa,<sup>11</sup> whose origin of  $\rho(T)$  is under debate. The resistivity is influenced by not only the spin fluctuations predicted by the SCR theory but also the band structure and disorder in the crystal. Therefore, an elaborate theory considering the actual band structure and the inherent effect of disorder is needed to explain the observed resistivity. Nevertheless, the electron correlation effect in  $\text{FeGa}_3$  is not significant compared with  $\text{FeSi}$ ,<sup>32</sup> because of the absence of impurity induced density of states at the Fermi level indicated by the extremely small  $\gamma$  value of 0.03 mJ/K<sup>2</sup>mol.<sup>28</sup> It is noteworthy that  $\text{FeGa}_3$  with such a weak correlation effect exhibits the QCB near the critical point from the nonmagnetic state to the FM ground state. The QCB may be induced by strong spin fluctuations due to the disturbance in the Fe 3*d*- Ga 4*p* hybridization. In order to clarify this point, neutron scattering studies on  $\text{FeGa}_{3-y}\text{Ge}_y$  single crystals are highly desirable.

## V. CONCLUSION

The effect of electron doping on the electronic and magnetic states of a diamagnetic semiconductor  $\text{FeGa}_3$  with a rather large band gap of 0.5 eV has been studied using single crystalline samples  $\text{Fe}_{1-x}\text{Co}_x\text{Ga}_3$  and  $\text{FeGa}_{3-y}\text{Ge}_y$ . A semiconductor-metal transition in  $\text{Fe}_{1-x}\text{Co}_x\text{Ga}_3$  occurs at  $x = 0.23$ , whereas no magnetic order is induced in the whole range  $0 \leq x \leq 1$ . These observations can be explained by the gradual change of the band structure in the rigid-band frame. On the other hand, substitution of Ge for Ga in  $\text{FeGa}_{3-y}\text{Ge}_y$  at a small value  $y = 0.006$  yields metallic conduction, and further doping at  $y = 0.13$  induces weak ferromagnetism. The  $\gamma$  value as a function of  $y$  exhibits a large peak of 70 mJ/K<sup>2</sup>molFe at  $y = 0.09$ . The critical concentration  $y_c = 0.13$  for the ferromagnetism is rather small, in spite of the fact that the band gap of 0.5 eV is one order of magnitude larger than the gap sizes in  $\text{FeSi}$  and  $\text{FeSb}_2$ . The FM quantum critical behaviors are manifested as  $C/T \propto -\ln T$  and  $M/B \propto T^{-4/3}$  near the critical concentration of  $y_c = 0.13$  in  $\text{FeGa}_{3-y}\text{Ge}_y$ . This FM instability is attributed to strong electron correlations, which are induced by the disturbance in the Fe 3*d* - Ga 4*p* hybridization by substituting Ge for Ga. Finally, we note that this system serves as a model system to investigate the FM instability in the simultaneous presence of disorder and electronic interaction, a problem that has been theoretically investigated.<sup>52</sup>



## ACKNOWLEDGMENTS

We thank F. Iga and for fruitful discussions. The magnetization and specific heat measurements were performed at N-BARD, Hiroshima University. This work was supported by the Scientific Research (A) (18204032) from MEXT, Japan.

---

\* kumeo@sci.hiroshima-u.ac.jp

- <sup>1</sup> V. Jaccarino, G. K. Wertheim, J. H. Wernick, L. R. Walker, and S. Aarj, Phys. Rev. **160**, 476 (1967).
- <sup>2</sup> J. Beille, J. Voiron, and M. Roth, Solid State Commun. **47**, 399 (1983).
- <sup>3</sup> Z. Schlesinger, Z. Fisk, H.-T. Zhang, M. B. Maple, J. F. DiTusa, and G. Aeppli, Phys. Rev. Lett. **71**, 1748 (1993).
- <sup>4</sup> D. Mandrus, J. L. Sarrao, A. Migliori, J. D. Thompson, and Z. Fisk, Phys. Rev. B **51**, 4763 (1995).
- <sup>5</sup> V. I. Anisimov, S. Y. Ezhov, I. S. Elfimov, I. V. Solovyev, and T. M. Rice, Phys. Rev. Lett. **76**, 1735 (1996).
- <sup>6</sup> S. Paschen, E. Felder, M. A. Chernikov, L. Degiorgi, H. Schwer, H. R. Ott, D. P. Young, J. L. Sarrao, and Z. Fisk, Phys. Rev. B **56**, 12916 (1997).
- <sup>7</sup> B. Buschinger, C. Geibel, F. Steglich, D. Mandrus, D. Young, J. L. Sarrao, and Z. Fisk, Physica B **230–232**, 784 (1997).
- <sup>8</sup> V. I. Anisimov, R. Hlubina, M. A. Korotin, V. V. Mazurenko, T. M. Rice, A. O. Shorikov, and M. Sigrist, Phys. Rev. Lett. **89**, 257203 (2002).
- <sup>9</sup> T. Saso and K. Urasaki, J. Phys. Chem. Solids **63**, 1475 (2002).
- <sup>10</sup> S. Yeo, S. Nakatsuji, A. D. Bianchi, P. Schlottmann, Z. Fisk, L. Balicas, P. A. Stampe, and R. J. Kennedy, Phys. Rev. Lett. **91**, 046401 (2003).
- <sup>11</sup> Y. Onose, N. Takeshita, C. Terakura, H. Takagi, and Y. Tokura, Phys. Rev. B **72**, 224431 (2005).
- <sup>12</sup> M. Arita, K. Shimada, Y. Takeda, M. Nakatake, H. Namatame, M. Taniguchi, H. Negishi, T. Oguchi, T. Saitoh, A. Fujimori, and T. Kanomata, Phys. Rev. B **77**, 205117 (2008).

- <sup>13</sup> H. Yamaoka, M. Matsunami, R. Eguchi, Y. Ishida, N. Tsujii, Y. Takahashi, Y. Senba, H. Ohashi, and S. Shin, Phys. Rev. B **78**, 045125 (2008).
- <sup>14</sup> D. Plencner and R. Hlubina, Phys. Rev. B **79**, 115106 (2009).
- <sup>15</sup> J. Imriška and R. Hlubina, Phys. Rev. B **84**, 195144 (2011).
- <sup>16</sup> C. Petrovic, J. W. Kim, S. L. Bud'ko, A. I. Goldman, P. C. Canfield, W. Choe and G. J. Miller, Phys. Rev. B **67**, 155205 (2003).
- <sup>17</sup> C. Petrovic, Y. Lee, T. Vogt, N. Dj. Lazarov, S. L. Bud'ko, and P. C. Canfield, Phys. Rev. B **72**, 045103 (2005).
- <sup>18</sup> A. Perucchi, L. Degiorgi, R. Hu, C. Petrovic, and V. F. Mitrovic, Eur. Phys. J. B **54**, 175 (2006).
- <sup>19</sup> A. Bentien, G. K. H. Madsen, S. Johnsen, and B. B. Iversen, Phys. Rev. B **74**, 205105 (2006).
- <sup>20</sup> R. Hu, V. F. Mitrovic, and C. Petrovic, Phys. Rev. B **74**, 195130 (2006).
- <sup>21</sup> R. Hu, R. P. Hermann, F. Grandjean, Y. Lee, J. B. Warren, V. F. Mitrovic, and C. Petrovic, Phys. Rev. B **76**, 224422 (2007).
- <sup>22</sup> A. Bentien, S. Johnsen, G. K. H. Madsen, B. B. Iversen, and F. Steglich, EuroPhys. Lett. **80**, 17008 (2007).
- <sup>23</sup> C. Dasarathy and W. Hume-Rothery, Proc. R. Soc. London, Ser. A **286**, 141 (1965).
- <sup>24</sup> U. Häussermann, M. Boström, P. Viklund, Ö. Rapp, and T. Björnängen, J. Solid State Chem. **165**, 94 (2002).
- <sup>25</sup> Y. Amagai, A. Yamamoto, T. Iida, and Y. Takanashi, J. Appl. Phys. **96**, 5644 (2004).
- <sup>26</sup> Y. Imai and A. Watanabe, Intermetallics **14**, 722 (2006).
- <sup>27</sup> N. Tsujii, H. Yamaoka, M. Matsunami, R. Eguchi, Y. Ishida, Y. Senba, H. Ohashi, S. Shin, T. Furubayashi, H. Abe, and H. Kitazawa, J. Phys. Soc. Jpn. **77**, 024705 (2008).
- <sup>28</sup> Y. Hadano, S. Narazu, Marcos A. Avila, T. Onimaru, and T. Takabatake, J. Phys. Soc. Jpn. **78**, 013702 (2009).
- <sup>29</sup> E. M. Bittar, C. Capan, G. Seyfarth, P. G. Pagliuso, and Z. Fisk, J. Phys.: Conf. Ser. **200**, 012014 (2010).
- <sup>30</sup> Z. P. Yin and W. E. Pickett, Phys. Rev. B **82**, 155202 (2010).
- <sup>31</sup> N. Haldolaarachchige, A. B. Karki, W. Adam Phelan, Y. M. Xiong, R. Jin, Julia Y. Chan, S. Stadler, and D. P. Young, J. Appl. Phys. **109**, 103712 (2011).

- <sup>32</sup> M. Arita, K. Shimada, Y. Utsumi, O. Morimoto, H. Sato, H. Namatame, M. Taniguchi, Y. Hadano, and T. Takabatake, Phys. Rev. B **83**, 245116 (2011).
- <sup>33</sup> V. G. Storchak, J. H. Brewer, R. L. Lichti, R. Hu, and C. Petrovic, J. Phys.: Condens. Matter. **24**, 185601 (2012).
- <sup>34</sup> Y. Nishino, M. Kato, S. Asano, K. Soda, M. Hayasaki, and U. Mizutani, Phys. Rev. Lett. **79**, 1909 (1997).
- <sup>35</sup> D. N. Basov, F. S. Pierce, P. Volkov, S. J. Poon, and T. Timusk, Phys. Rev. Lett. **73**, 1865 (1994).
- <sup>36</sup> D. Bogdanov, K. Winzer, I. A. Nekrasov, and T. Pruschke, J. Phys. Condens. Matter **19**, 232202 (2007).
- <sup>37</sup> T. Takabatake, F. Iga, T. Yoshino, Y. Echizen, K. Katoh, K. Kobayashi, M. Higa, N. Shimizu, Y. Bando, G. Nakamoto, H. Fujii, K. Izawa, T. Suzuki, T. Fujita, M. Sera, M. Hiroi, K. Maezawa, S. Mock, H. v. Löhneysen, A. Brückl, K. Neumaier, K. Andres, J. Magn. Magn. Mater. **177-181**, 277 (1998).
- <sup>38</sup> J. Kuneš and V. I. Anisimov, Phys. Rev. B **78**, (2008) 033109.
- <sup>39</sup> D. Zur, D. Menzel, I. Jursic, J. Schoenes, L. Patthey, M. Neef, K. Doll, and G. Zwicknagl, Phys. Rev. B **75**, 165103 (2007).
- <sup>40</sup> M. Klein, D. Zur, D. Menzel, J. Schoenes, K. Doll, J. Roder, and F. Reinert, Phys. Rev. Lett. **101**, 046406 (2008).
- <sup>41</sup> A. V. Lukoyanov, V. V. Mazurenko, V. I. Anisimov, M. Sigrist, and T. M. Rice, Eur. Phys. J. B **53**, 205 (2006).
- <sup>42</sup> P. Viklund, S. Lidin, P. Berastegui, and U. Häussermann, J. Solid State Chem. **165**, 100 (2002).
- <sup>43</sup> T. Sakakibara, H. Mitamura, T. Tayama, and H. Amitsuka, Jpn. J. Appl. Phys. **33**, 5067 (1994).
- <sup>44</sup> S. Blundell, in *Magnetism in Condensed Matter* (Oxford University Press, New York, 2001).
- <sup>45</sup> A. J. Millis, Phys. Rev. B **48**, 7183 (1993).
- <sup>46</sup> T. Moriya, in *Spin Fluctuation in Itinerant Electron Magnetism* (Springer-Verlag, Berlin, 1985).
- <sup>47</sup> J.-Y. Son, K. Okazaki, T. Mizokawa, A. Fujimori, T. Kanomata, and R. Note, Phys. Rev. B **68**, 134447 (2003).
- <sup>48</sup> V. Dorin and P. Schlottmann, Phys. Rev. B **46**, 10800 (1992).
- <sup>49</sup> G. R. Stewart, Rev. Mod. Phys. **73**, 797 (2001); K. Umeo, H. Kadomatsu, and T. Takabatake, J. Phys.: Condens. Matter **8**, 9743 (1996).

- <sup>50</sup> F. Grosche, F. M., S. R. Julian, N. D. Mathur, and G. G. Lonzarich, *Physica B* **223-224**, 50 (1996).
- <sup>51</sup> M. Nicklas, M. Brando, G. Knebel, F. Mayr, W. Trinkl, and A. Loidl, *Phys. Rev. Lett.* **82**, 4268 (1999).
- <sup>52</sup> P. B. Chakraborty, K. Byczuk, and D. Vollhardt, *Phys. Rev. B* **84**, 155123 (2011).

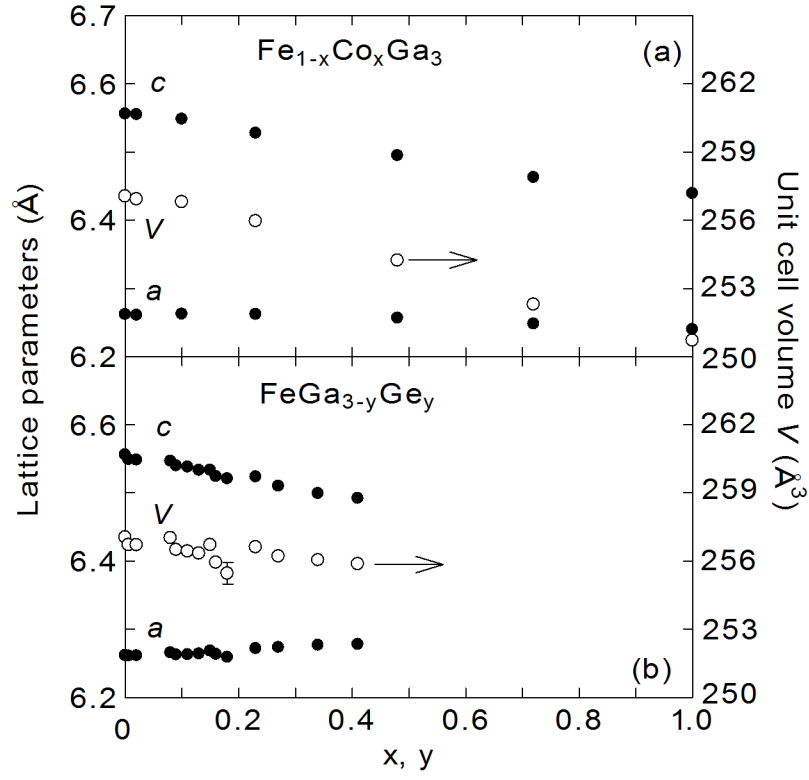


FIG. 1. Lattice parameters and unit cell volume of  $\text{Fe}_{1-x}\text{Co}_x\text{Ga}_3$  (a) and  $\text{FeGa}_{3-y}\text{Ge}_y$  (b) as a function of concentrations  $x$  and  $y$ .

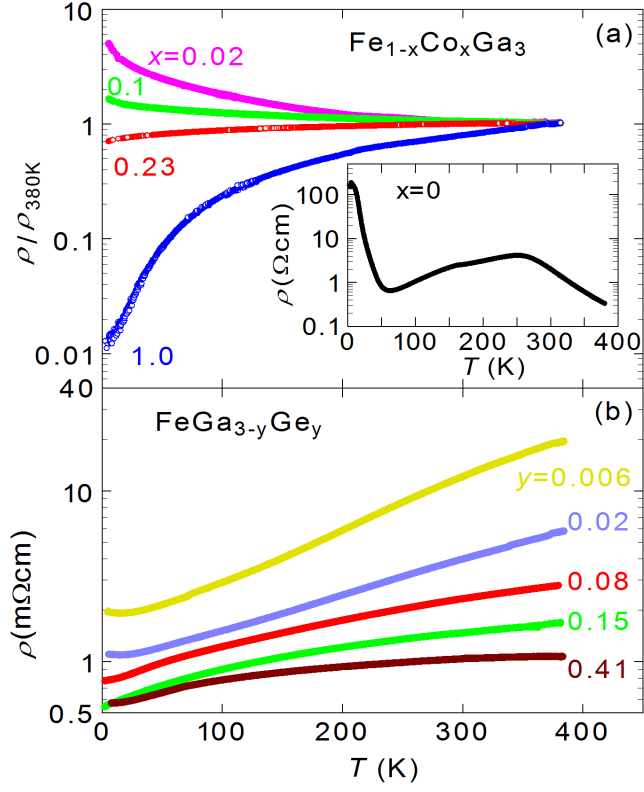


FIG. 2. Temperature dependence of electrical resistivity  $\rho$  for  $\text{Fe}_{1-x}\text{Co}_x\text{Ga}_3$  (a) and  $\text{FeGa}_{3-y}\text{Ge}_y$  (b). The resistivity of  $\text{Fe}_{1-x}\text{Co}_x\text{Ga}_3$  is normalized by the value at 380 K. The inset shows the resistivity for  $\text{FeGa}_3$  ( $x = 0$ ).<sup>28</sup>

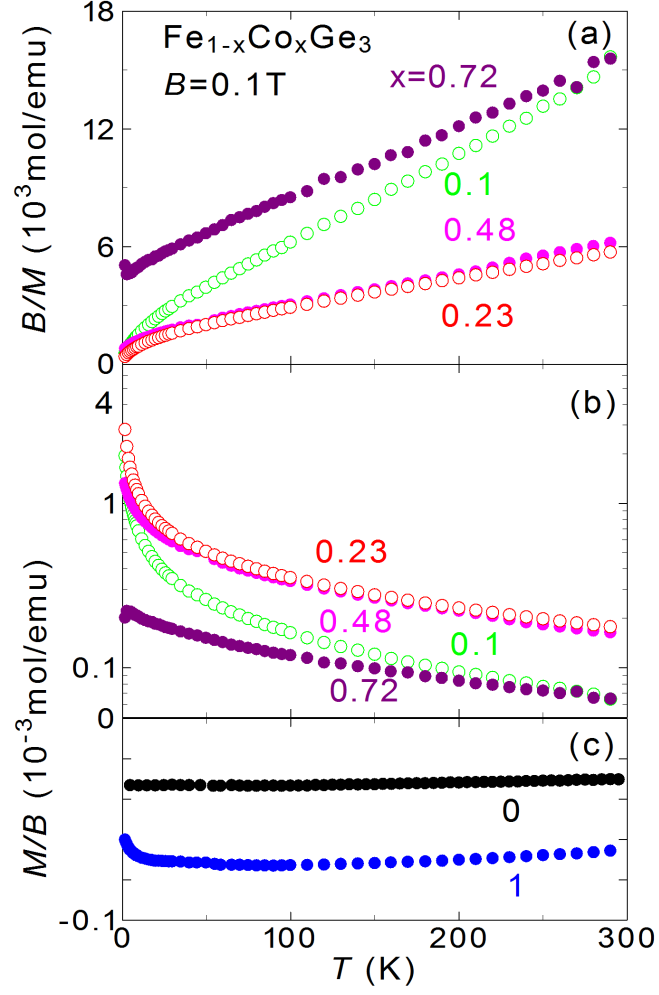


FIG. 3. Temperature dependence of magnetic susceptibility  $M/B$  (b) and inverse magnetic susceptibility  $B/M$  (a) of  $\text{Fe}_{1-x}\text{Co}_x\text{Ga}_3$

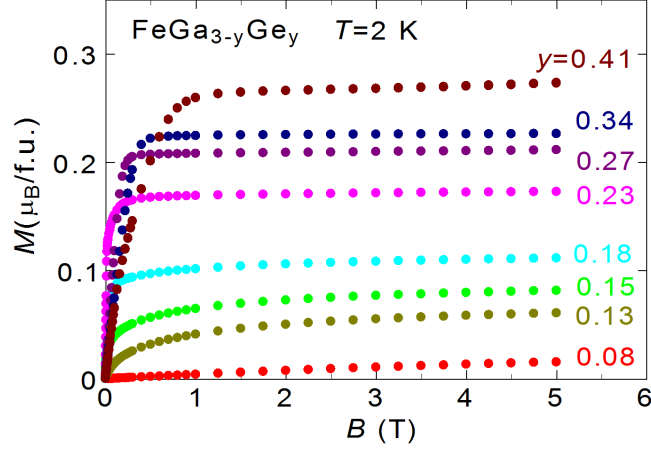


FIG. 4. Isothermal magnetization curves of  $\text{FeGa}_{3-y}\text{Ge}_y$  at 2 K.

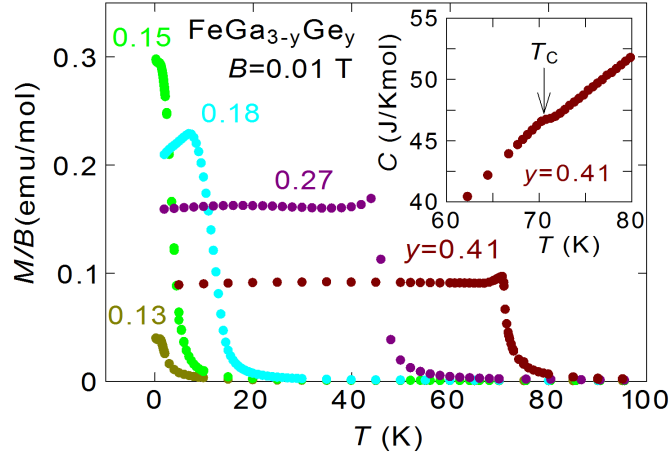


FIG. 5. Temperature dependence of magnetic susceptibility  $M/B$  of  $\text{FeGa}_{3-y}\text{Ge}_y$  for  $y \geq 0.13$  where ferromagnetic transitions are observed. The inset shows the specific heat of  $\text{FeGa}_{3-y}\text{Ge}_y$  for  $y = 0.41$  near  $T_C$ .



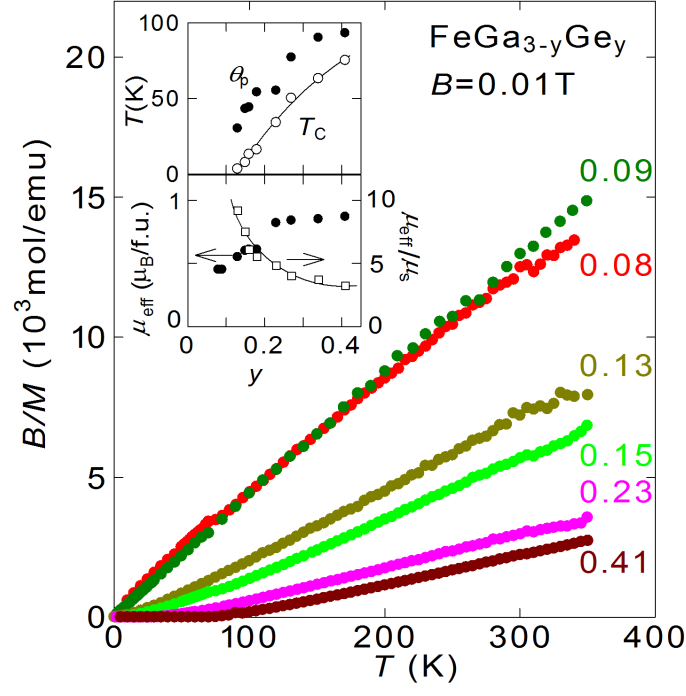


FIG. 6. Temperature dependence of the inverse magnetic susceptibility  $B/M$  of  $\text{FeGa}_{3-y}\text{Ge}_y$ . The upper and lower panels of the inset show the paramagnetic Curie temperature  $\theta_P$  and ferromagnetic transition temperature  $T_C$ , and effective magnetic moments  $\mu_{\text{eff}}$  and the Rhodes-Wohlfarth value  $\mu_{\text{eff}}/\mu_s$ , respectively, as a function of  $y$ .

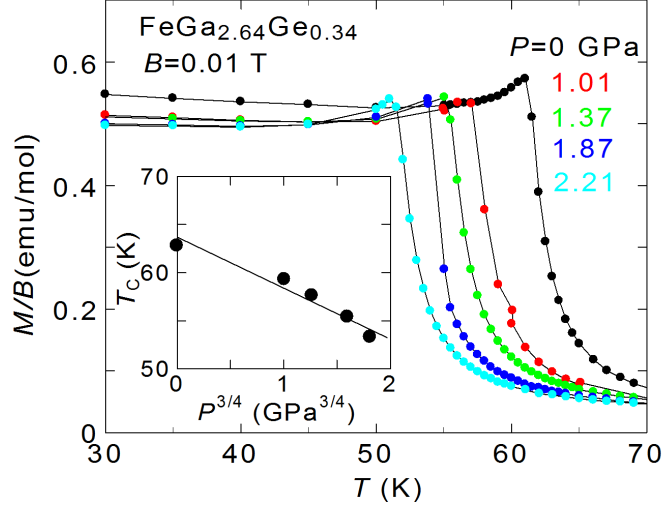


FIG. 7. Temperature dependence of magnetic susceptibility  $M/B$  of  $\text{FeGa}_{3-y}\text{Ge}_y$  for  $y = 0.34$  under various pressures  $P$ . The inset shows  $T_C$  as a function of  $P^{3/4}$ .

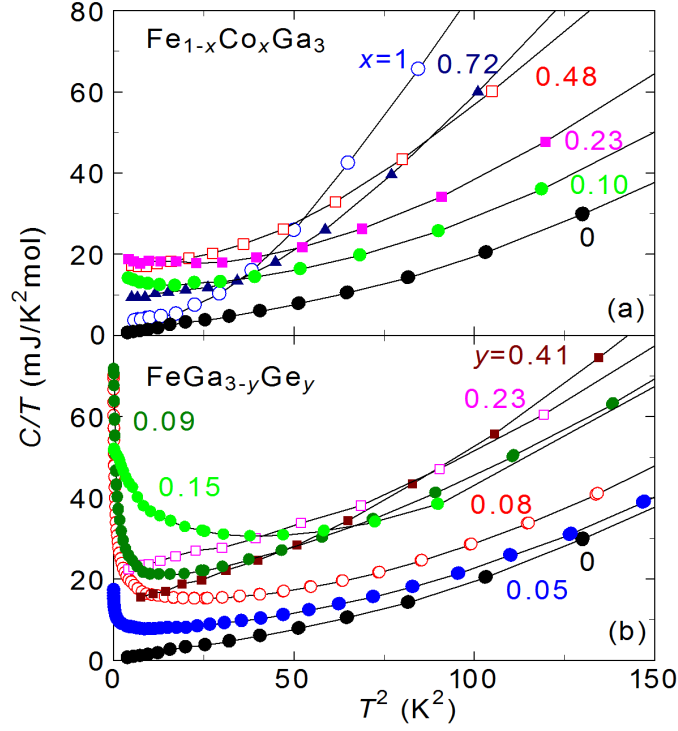


FIG. 8. The specific heat divided by temperature  $C/T$  for  $\text{Fe}_{1-x}\text{Co}_x\text{Ga}_3$  (a) and  $\text{FeGa}_{3-y}\text{Ge}_y$  (b) as a function of  $T^2$ .

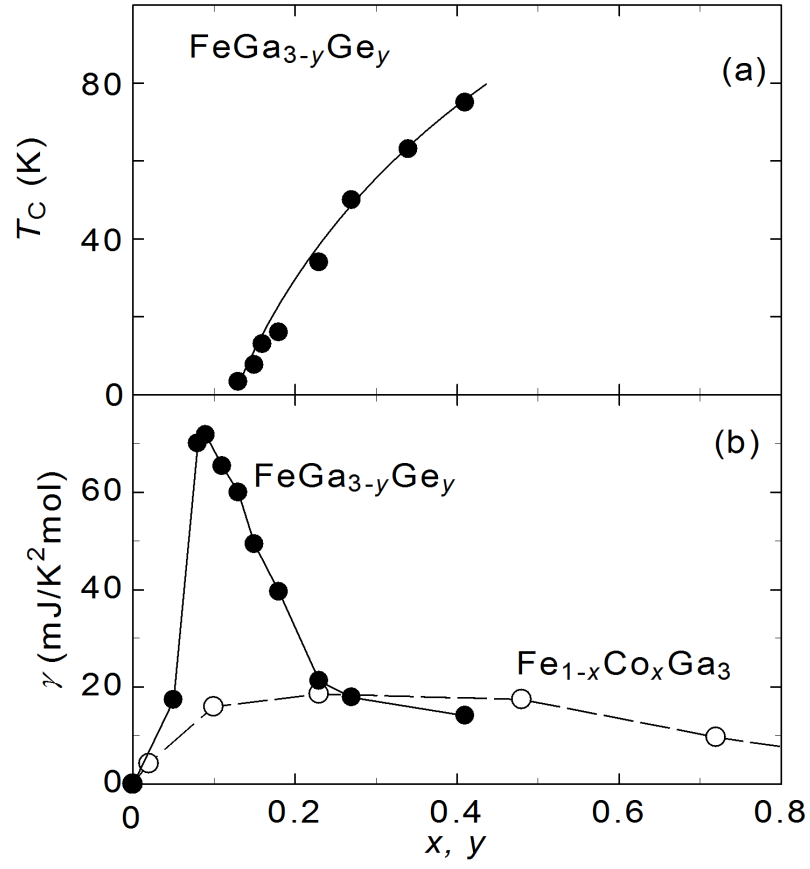


FIG. 9. Ferromagnetic transition temperature  $T_C$  (a) and electronic specific heat coefficient  $\gamma$  (b) for  $\text{Fe}_{1-x}\text{Co}_x\text{Ga}_3$  and  $\text{FeGa}_{3-y}\text{Ge}_y$  as a function of  $x$  and  $y$ .

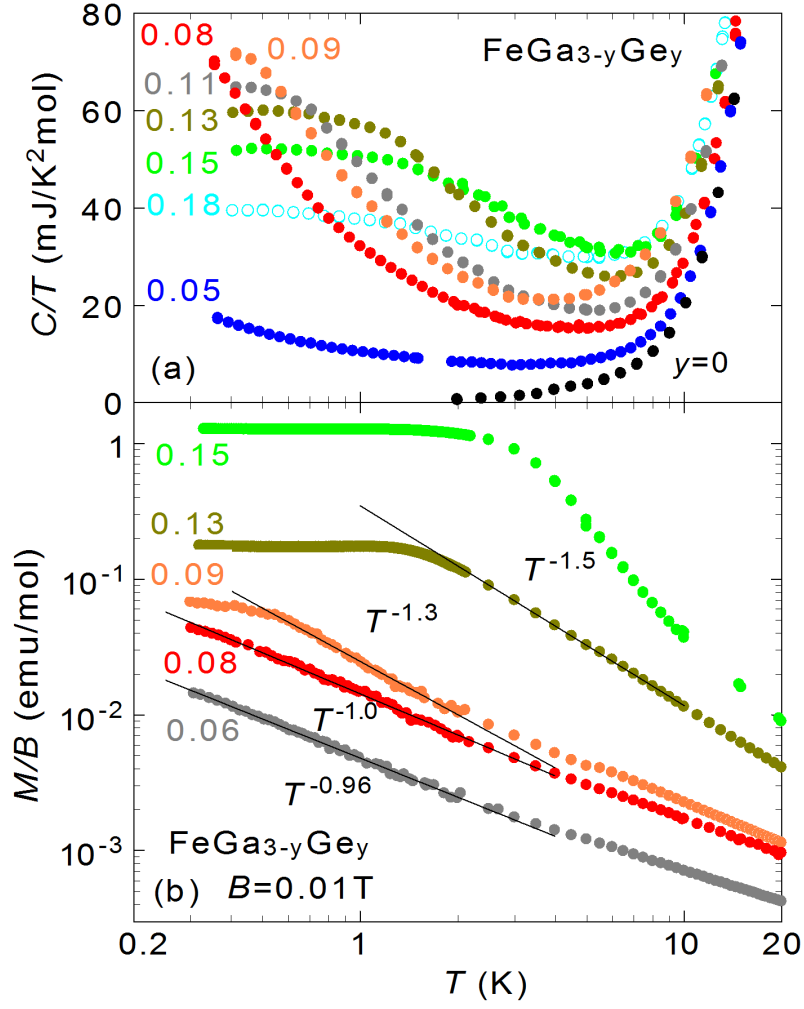


FIG. 10. Logarithmic temperature dependence of  $C/T$  (a) and  $M/B$  (b) for FeGa<sub>3-y</sub>Ge<sub>y</sub> near the FM instability.

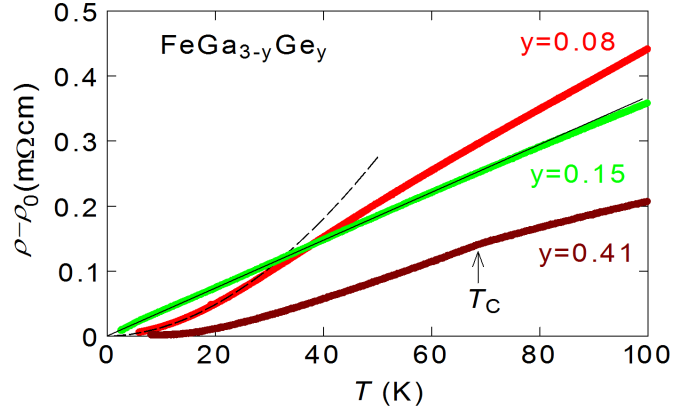


FIG. 11. Temperature dependence of electrical resistivity  $\rho$  of  $y = 0.08$ ,  $0.15$ , and  $0.41$  for  $\text{FeGa}_{3-y}\text{Ge}_y$ . The  $\rho(T)$  data for  $y = 0.08$ , and  $0.15$  were fitted by  $\rho - \rho_0 \propto T^{1.9}$  (broken line) and  $\rho - \rho_0 \propto T$  (solid line), respectively.